The Journal of Immunology

Cyclooxygenase-2 Inhibitor Enhances the Efficacy of a Breast Cancer Vaccine: Role of IDO

Gargi D. Basu, Teresa L. Tinder, Judy M. Bradley, Tony Tu, Christine L. Hattrup, Barbara A. Pockaj and Pinku Mukherjee

J Immunol 2006; 177:2391-2402; ;
doi: 10.4049/jimmunol.177.4.2391
http://www.jimmunol.org/content/177/4/2391

The Journal of Immunology is published twice each month by
The American Association of Immunologists, Inc.,
1451 Rockville Pike, Suite 650, Rockville, MD 20852

Print ISSN: 0022-1767 Online ISSN: 1550-6606.

Cyclooxygenase-2 Inhibitor Enhances the Efficacy of a Breast Cancer Vaccine: Role of IDO[1]

Gargi D. Basu, Teresa L. Tinder, Judy M. Bradley, Tony Tu, Christine L. Hattrup, Barbara A. Pockaj, and Pinku Mukherjee[2]

We report that administration of celecoxib, a specific cyclooxygenase-2 (COX-2) inhibitor, in combination with a dendritic cell-based cancer vaccine significantly augments vaccine efficacy in reducing primary tumor burden, preventing metastasis, and increasing survival. This combination treatment was tested in MMTV-PyV MT mice that develop spontaneous mammary gland tumors with metastasis to the lungs and bone marrow. Improved vaccine potency was associated with an increase in tumor-specific CTLs. Enhanced CTL activity was attributed to a significant decrease in levels of tumor-associated IDO, a negative regulator of T cell activity. We present data suggesting that inhibiting COX-2 activity in vivo regulates IDO expression within the tumor microenvironment; this is further corroborated in the MDA-MB-231 human breast cancer cell line. Thus, a novel mechanism of COX-2-induced immunosuppression via regulation of IDO has emerged that may have implications in designing future cancer vaccines. ***The Journal of Immunology,*** **2006, 177: 2391–2402.**

There has recently been great interest in cancer vaccines, which have the potential of controlling disease, prolonging time to recurrence, and ultimately serving as a preventive measure. In breast cancer, surgical resection provides a good prognosis for locally confined tumors, but patients with advanced stage disease are at high risk of relapse, emphasizing the need for additional treatment modalities. However, most cancer vaccines tested to date have shown limited clinical efficacy. An essential reason for this is that CTLs directed against the tumor become functionally inactive when exposed to the tumor microenvironment (1, 2). Immune escape, the ability of tumor cells to avoid destruction by the host immune system, is a major obstacle that must be addressed in designing and delivering a successful cancer vaccine. Although immune therapy has low toxicity and elicits antitumor immune responses, these approaches so far have failed to generate significant clinical responses (3–7).

The rationale for this study stems from the our previous work describing the failure of CTLs directed against tumor-associated Ags to cure a developing tumor (1, 8–10). This has been attributed to a number of immune evasion mechanisms used by the tumor, and which are well documented in humans. These include but are not restricted to release of immunosuppressive factors such as cyclooxygenase-2 (COX-2),[3] PGE_2, TGF-β2, and IL-10, all of which may render the CTLs cytolytically anergic (2, 11).

The breast tumor microenvironment is characterized by high expression of immunosuppressive factors including COX-2 and its product, PGE_2 (2, 12). COX-2 affects multiple pathways involved in tumorigenesis, including angiogenesis, invasion, and tumor-induced immune suppression (13, 14). It is recognized that COX-2 induces many of its effects through PGE_2, which targets both CTL and Th lymphocyte functions by inducing the release of immunosuppressive factors that favor tumor cell proliferation and angiogenesis (15, 16) (12, 17, 18). Thus, PGE_2 could directly block the defense mechanism against cancer and thereby promote cancer growth (15, 19). Recently, it has been shown that PGE_2 receptor, EP2, is absolutely required for COX-2 induced mammary carcinogenesis, making this a critical PG in breast cancer (20). Indeed, we observe functional impairment of adoptively transferred CTLs within the growing tumor microenvironment, which is heavily loaded with PGE_2 (2, 10). Thus, we hypothesize that the tumor microenvironment needs to be manipulated to overcome/decrease the immunosuppression. We have shown that COX-2 and PGE_2 overexpression is associated with impaired immune cell function in breast cancer patients and may be linked to metastatic potential (12). COX-2 inhibition therefore represents a useful approach for prevention and/or treatment of breast cancer in combination with either conventional or novel therapies. Studies with specific inhibitors of COX-2 have shown significant effects in reducing the incidence and progression of tumors in both animal models and cancer patients (21–23). We have recently demonstrated that treatment of a mouse model of metastatic breast cancer with the specific COX-2 inhibitor celecoxib decreased tumor cell proliferation and angiogenesis, while increasing tumor cell apoptosis accompanied by reduced activation of the cell survival kinase protein kinase B (PKB)/Akt, and up-regulation of the proapoptotic protein Bax (24). These published data provide us the immunological rationale for using COX-2 inhibition combined with immune-based therapy. This is a novel concept that has not been published in an appropriate mouse model of spontaneous tumor. The objective of this study was to determine whether inhibiting the mediators of immune-suppression such as COX-2/PGE_2 within the tumor microenvironment (in a spontaneously growing tumor-bearing host) could enhance the efficacy of targeted immune therapy (vaccine).

Mayo Clinic College of Medicine, and Mayo Clinic Arizona, Scottsdale, AZ 85259

Received for publication December 30, 1999. Accepted for publication June 2, 2006.

The costs of publication of this article were defrayed in part by the payment of page charges. This article must therefore be hereby marked *advertisement* in accordance with 18 U.S.C. Section 1734 solely to indicate this fact.

[1] This work was funded by the Susan G. Komen Breast Cancer Foundation and Mayo Foundation.

[2] Address correspondence and reprint requests to Dr. Pinku Mukherjee, Cellular Immunology Laboratory, Mayo Clinic School of Medicine, 13400 East Shea Boulevard, Scottsdale, AZ 85259. E-mail address: mukherjee.pinku@mayo.edu

[3] Abbreviations used in this paper: COX-2, cyclooxygenase-2; DC, dendritic cell; TDLN, tumor draining lymph node; PI, propidium iodide; PGEM, PGE_2 metabolite; PTEN, phosphatase and tensin homolog deleted on chromosome 10; siRNA, small interfering RNA; IHC, immunohistochemistry; PCNA, proliferating cell nuclear Ag; CI, confidence interval; PKB, protein kinase B.

0022-1767/06/$02.00

In this manuscript, we have addressed this issue by using the combination of a tumor-specific vaccine in combination with COX-2 inhibition with the hopes of improving the efficacy of tumor-targeted immune therapy.

Although inhibition of COX-2 makes a promising target for augmenting vaccine efficacy, it is not clear how COX-2 and PGE_2 suppress CTLs within the tumor microenvironment. In this study, we show that celecoxib treatment in a mouse model of spontaneous mammary gland tumorigenesis attenuates expression of IDO. IDO catalyzes the conversion of L-tryptophan to L-kynurenine, the rate-limiting step in tryptophan catabolism (25–27), and has recently been established as a major player in T cell suppression and induction of immune tolerance to tumors (25, 26, 28–30). By depleting tryptophan, IDO blocks proliferation and activation of T lymphocytes, which are particularly sensitive to loss of this essential amino acid (31, 32). In vivo, IDO maintains maternal tolerance toward the fetus during pregnancy (33) and participates in suppressing T cell responses to MHC-mismatched allografts (34, 35). IDO activity is increased under pathological conditions including tumor development (25, 36), and it is overexpressed in many tumors and on tolerizing APCs (25, 26, 29, 37–39). Transfection with IDO renders tumor cell lines immunosuppressive (32), and treatment with the competitive IDO inhibitor 1MT significantly delays tumor outgrowth in a model of lung carcinoma (39).

The importance of IDO in cancer progression and therapy is not fully understood. Accurate preclinical models of tumorigenesis are required to test IDO and other potential therapeutic targets. As a model of mammary oncogenesis, we used mice carrying the polyomavirus middle T Ag driven by the mouse mammary tumor virus promoter (PyV MT mice) (40–42). This oncogene is active throughout all stages of mammary gland development, resulting in widespread transformation and production of multifocal mammary adenocarcinomas by 9–10 wk of age, which metastasize to the lungs and bone marrow by 20 wk (10, 43). One hundred percent of female mice get tumors and, due to the extremely powerful nature of the oncogene, die by 18–24 wk of age. In this study, we report a 2- to 3-fold increase in the survival of PyV MT mice after treatment with either a dendritic cell (DC)-based vaccine plus celecoxib alone or vaccine plus celecoxib and low-dose chemotherapy. These combination treatments successfully enhance antitumor immunity, decrease tumor burden, and abrogate lung metastasis. Furthermore, we establish that tumor-induced COX-2 regulates the expression of IDO. Our data suggest that disrupting COX-2 in mammary tumors slows tumor progression and reduces immune escape, and that inhibiting either COX-2 or its downstream target IDO may be a powerful strategy to include in future antitumor vaccine regimens.

Materials and Methods

Generation of PyV MT mouse model

PyV MT oncogenic mice were originally a gift from Dr. W. J. Muller (McGill University, Toronto, Canada) (40). PyV MT male mice were mated to C57BL/6 mice to maintain the PyV MT mice as heterozygous. Approximately 50% of the pups carry the oncogene and, out of that, ~50% are females that develop mammary gland adenocarcinomas and are used for the experiments. PCR was used to routinely identify the PyV MT oncogene. PCR was conducted as previously described (10). Primer pairs for PyV MT transgene are 5′-AGTCACTGCTACTGCACCCAG-3′ (bp 282–302) and 5′-CTCTCCTCAGTTCCTCGCTCC-3′ (bp 817–837). The amplification program for PyV MT consisted of one cycle of 5 min at 95°C and 40 cycles of 30 s at 95°C, 1 min at 61°C, and 30 s at 72°C followed by one cycle of 10 min at 72°C. The PCR product was analyzed by size fractionation through a 1% agarose gel. Amplification of PyV MT gene results in a 480-bp fragment. All mice are congenic on the C57/BL6 background at $N \geq 10$. All mice were bred and maintained in specific pathogen-free conditions in the Mayo Clinic Scottsdale Natalie Schafer Transgenic Animal Facility. Experimental procedures using animals were conducted according to Institutional Animal Care and Use Committee (IACUC) guidelines.

Preparation of vaccine

DCs were generated from bone marrow cells derived from 6- to 8-wk-old wild-type C57BL/6 according to the method described (44). PyV MT tumors were dissected from 15-wk-old PyV MT mice that had a large tumor burden. Tumor lysates were made in tissue lysis buffer containing 20 mM HEPES, 0.15 M NaCl, and 1% Triton X-100 supplemented with 80 μl/ml phosphatase inhibitor mixture II (P-5726; Sigma-Aldrich) and 10 μl/ml complete protease inhibitor mixture (Boehringer Mannheim). Immature DCs were incubated with 20 μg/ml tumor lysate for 24 h followed by LPS (1 μg/ml) for another 24 h to mature the DCs. Optimal concentration of tumor lysate was determined by incubating DCs with varying concentrations of the lysate and then assessing the cell viability and DC phenotype. DC phenotype was analyzed by two-color flow cytometry for maturation surface markers including CD11c, MHC class II, CD86, CD80, CD40, and CD54; Abs were purchased from BD Pharmingen. Flow cytometric analysis was done on a BD Biosciences FACScan using the CellQuest program.

Study design

Three-week-old mice were injected intradermally with 1×10^7 lysate-fed DCs (vaccine). Immunizations were repeated every 3 wk until termination of experiment at 21 wk. Starting at 6 wk of age, celecoxib was orally gavaged at 10 mg/kg dosage dissolved in DMSO every day (5 days on with 2 days off) for the entire length of the study as described previously (24). No treatment was given on weekends. Control mice were gavaged with DMSO. Cyclophosphamide was administered i.p. to the mice starting at 9 wk of age at 50 mg/kg dose every 3 wk. This dose of cyclophosphamide was previously found to be suboptimal with no effect on the tumor burden or survival in the PyV MT mice (data not shown). The treatment arms include the following: 1) DMSO as vehicle (control), 2) vaccine, 3) celecoxib, 4) vaccine plus celecoxib, and 5) vaccine plus celecoxib plus chemotherapy. Other treatment groups that were enrolled but not shown in the results are the following: celecoxib plus chemotherapy; vaccine plus chemotherapy; untreated control; and chemotherapy alone. Twenty mice were enrolled in each treatment arm, half of which were kept for survival and the other half for tumor burden and endpoint analysis. Upon sacrifice, tumor draining lymph node (TDLN) and mammary gland tumors were dissected. Part of the tumor was used to prepare lysates for protein analysis and part was used for immunohistochemistry (IHC) and flow cytometry. We compared the immune responses that developed with treatment, and used tumor onset, tumor burden, and overall survival as the endpoints for determining the clinical effectiveness of the vaccine.

Analysis of PyV MT tumors

Mice were palpated every week starting at 10 wk of age until sacrifice at 21 wk. Palpable tumors were measured by calipers and tumor weight was calculated according to the following formula: grams = (length in centimeters $\times$ $(\text{width})^2$)/2 (45). In accordance with IACUC regulation, all survival mice were sacrificed when tumors reached 10% of body weight. Mice were carefully observed for signs of ill health, including lethargy, abdominal distention, failure to eat or drink, marked weight loss, and hunched posture.

Analysis of PGE_2 in serum

PGE_2 levels in the serum were determined using a specific ELISA kit for PGE_2 metabolite (PGEM) (13,14-dihydro-15-keto-PGA_2) (Cayman Pharmaceuticals). Manufacturer's recommended protocols were followed. Serum was diluted appropriately to ensure that readings were within the limits of accurate detection. Results are expressed as picograms of PGEM/milliliter of serum.

IFN-γ ELISPOT assay

From the TDLNs, $CD4^+$ and $CD8^+$ T cells were isolated using the MACS (Miltenyi Biotec). IFN-γ ELISPOT assay was performed using capture IFN-γ Ab as recommended by the manufacturer (Mabtech). Autologous irradiated DCs pulsed with tumor lysate were used as stimulator cells and added at a responder to stimulator ratio of 10:1. Control wells contained T cells stimulated with DCs pulsed with irrelevant peptide. Spot numbers were determined using a computer-assisted video image analyzer by Zellnet Consulting. DCs pulsed with irrelevant peptides were used as control. Splenocytes from a C57BL/6 mice stimulated with Con A was used as positive control (data not shown).

^{51}Cr release assay

Determination of CTL activity was performed using a standard ^{51}Cr release method. CD8$^+$ T cells from TDLN were sorted and served as effector cells. Autologous irradiated DCs pulsed with tumor lysate were used as stimulator cells and coincubated with the effector cells at a effector:stimulator ratio of 10:1 for 48 h. Effector cells were then recovered and incubated with ^{51}Cr-labeled PyV MT tumor target cells at an E:T ratio of 100:1. Target cells were treated with 5 ng/ml IFN-γ (Amersham Biosciences) 1 day before the assay to up-regulate MHC class I surface expression and loaded with radioactivity (^{51}Cr; Amersham Biosciences) for 3 h. Effectors and targets were coincubated for 8 h. Radioactive ^{51}Cr released at the end of 8 h was determined using the Topcount microscintillation counter (Packard Biosciences). Radioactivity was measured as cpm. Specific lysis was calculated according to the following formula: (experimental cpm − spontaneous cpm/complete cpm − spontaneous cpm) × 100. Spontaneous ^{51}Cr release in all experiments was 10–15% of complete ^{51}Cr release.

Analysis of apoptosis by flow cytometry

Part of the tumor tissue was dissociated to generate single-cell suspension by incubating in 5 mM EDTA solution for 1 h at 37°C incubator with 5% CO_2. Apoptosis was determined by staining single cells (1×10^6) with annexin V and propidium iodide (PI) using the BD Pharmingen apoptosis kit following the manufacturer's protocol. Staining was determined by flow cytometry. Viable cells exclude PI and are negative for annexin V staining, whereas early apoptotic cells stain positive for annexin V and are PI negative. Cells that are not viable due to apoptotic cell death stain positive for both annexin V and PI. Percent apoptotic cells were determined by CellQuest statistical analysis program as the cumulative percent cells that were stained positive for both PI and annexin V (upper right quadrant), and cells that were stained for annexin V only (lower right quadrant).

Western blot analysis

All tumor and DC lysates were made in tissue lysis buffer containing 20 mM HEPES, 0.15 M NaCl, and 1% Triton X-100 supplemented with 80 μl/ml phosphatase inhibitor mixture II (P-5726; Sigma-Aldrich) and 10 μl/ml complete protease inhibitor mixture (Boehringer Mannheim). Protein concentration was determined by BCA assay (Pierce) and lysates (100 μg/lane) resolved by SDS-PAGE on 10–15% resolving gels. Gels were blotted and probed for IDO, Bax, phosphatase and tensin homolog deleted on chromosome 10 (PTEN), survivin, and β-actin. All primary Abs were purchased from Santa Cruz Biochemicals and used at 1/200 dilutions. Appropriate secondary Abs were used. Densitometric analysis was performed on a Macintosh computer using the public domain Java image processing program ImageJ (developed at the National Institutes of Health and available at ⟨http://rsb.info.nih.gov/ij/index.html⟩) (46).

Small interfering RNA (siRNA) transfections

The human breast cancer cell line MDA-MB-231 (high COX-2 expression) was plated at a density of 225,000 cells/well in six-well plates and grown to 50% confluence. After 24 h, the cells were transfected with siRNA (COX-2 and nonspecific control) in lipofectamine 2000 transfection reagent (Invitrogen Life Technologies) according to the manufacturer's instruction. The COX-2-specific siRNA was purchased from Dharmacon. A nonspecific control (nonsilencing) siRNA synthesized by Dharmacon was used as control. Briefly, for each well, 10 μl of transfection reagent was incubated with 500 μl of OPTI-MEM medium for 5 min. Subsequently, the respective siRNA in OPTI-MEM medium was added to the transfection medium, resulting in a siRNA concentration of 50 nM, and added to the cells. Two days posttransfection, lysates were prepared and COX-2 and IDO protein expression was evaluated by Western blotting.

IHC: TUNEL, proliferating cell nuclear Ag (PCNA), IDO, COX-2, and CD8 staining

Part of the tumor was formalin fixed (10% neutral buffered formalin, pH 6.8–7.2; Fischer Scientific) and paraffin embedded, and 5-μm sections were prepared by the Mayo Clinic Scottsdale Histology Core Facility. After deparaffinization in xylene, rehydrating, PROTEINASE K pretreatment for Ag retrieval, and quenching with hydrogen peroxide, IHC was performed using the ApopTag Peroxidase in situ apoptosis detection kit (Serologicals Corporation). 3,3′-Diaminobenzidine was used as the chromagen and hematoxylin was used as counterstain. TUNEL-positive cells were examined under light microscopy and representative images were taken at ×200. For PCNA, IDO, COX-2, and CD8 staining, paraffin-embedded and 5-μm sections were subjected to Ag retrieval using the DakoCytomation Target Retrieval at 95°C for 40 min. Primary Ab (PCNA Ab; BD Biosciences; COX-2, IDO, and CD8 Abs; Santa Cruz Biochemicals) was used at 5 μg/ml for PCNA, and 1/200 dilution for the others at 4°C overnight and DakoCytomation anti-mouse secondary conjugated to HRP was used at 1/200 for 2 h at room temperature. Diaminobenzidine was used as the chromagen, and hematoxylin was used as counterstain.

All human breast cancer tissues were obtained from the Mayo Clinic Scottsdale and stained with anti-COX-2 (Santa Cruz Biotechnology) and anti-IDO (Chemicon International) Abs using the manufacturers' recommended staining protocol. Grading of the tumors was done according to the Nottingham and modified Bloom Richardson grading criteria. There were $n = 5$ for grade 1/3, $n = 5$ for grade 2/3, and $n = 4$ for grade 3/3. All were described as infiltrating ductal lobular carcinoma of the breast. Four specimens were described as lymph node positive (see Table II). Staining intensity was recorded on a scale of plus 1 to plus 4, with + being low staining intensity and ++++ being staining of the highest intensity. Pearson coefficient index was calculated to correlate COX-2 staining with IDO staining pattern. The Mayo Clinic Institutional Review Board approved this study.

Statistical analysis

All statistical analysis was conducted by the Mayo Clinic biostatistics core facility. Values of p are from the one-way ANOVA F test for comparing the treatment groups simultaneously and from the pairwise contrasts from a one-way ANOVA with Dunnett adjustment. Values of p for lung metastasis are from the Pearson χ^2 statistic and from Kruskal-Wallis test. All data are expressed as means ± SD of the mean. Kaplan-Meier's statistics and log-rank tests were performed to estimate significant differences in survival times. For survival data, the t test was used to determine whether there was any statistical difference in the survival weeks between the groups. A value of $p < 0.05$ was considered to be significant. For correlation analysis, Spearman rank correlation coefficient and weighted κ coefficient were calculated. To determine whether the effect of celecoxib and vaccine were additive or synergistic on tumor burden, CTL activity, and survival, data were analyzed using a general linear model with terms for celecoxib, vaccine, and the interaction between the two. The interaction is the effect of celecoxib and vaccine on the different measures (tumor burden, CTL activity, and survival). If there is a significant interaction ($p < 0.05$), then there is evidence that an independent variable (celecoxib or vaccine) is influenced by the presence of the other. The higher the interaction value, the greater is the synergy. If the value of interaction is ≤1, the interaction is deemed additive. A value >1 is a synergistic interaction. If p values were significant for the three different measures, then there was significant evidence that the effect of vaccine is influenced by the presence of the celecoxib (or vice versa).

Results

COX-2 inhibitor enhances the efficacy of a breast cancer vaccine

Celecoxib, when administered in combination with a DC-based breast cancer vaccine (treatment schema shown in Fig. 1*A*), significantly augments the effectiveness of the vaccine in reducing primary mammary gland tumor burden (Fig. 1*B*), preventing lung metastasis (Fig. 1*B*, *inset*), and increasing survival (Fig. 1*C*). Starting at age 3 wk, mice were injected s.c. every 3 wk with 1×10^7 DCs pulsed with autologous tumor lysate (vaccine). Celecoxib (10 mg/kg) was administered daily by oral gavage starting at age 6 wk. In addition, some mice received a suboptimal dose of cyclophosphamide (50 mg/kg) once every 3 wk by i.p. injection starting at age 9 wk (Fig. 1*A*). Chemotherapy was given 2 days before vaccine treatment. All treatment groups continued until age 21–23 wk, when mice were sacrificed for endpoint analysis. Although a significant decrease in primary tumor burden was observed in the celecoxib-alone and vaccine-alone groups ($p < 0.0001$ compared with control), the decrease was more pronounced in mice treated with vaccine plus celecoxib ($p = 0.0001$). Importantly, mice receiving combination treatment did not develop the florid lung metastases seen in control mice (Fig. 1*B*, *inset*). Tumor burden remained low when cyclophosphamide was added to the treatment regimen ($p < 0.0001$ compared with control) with no significant difference between the vaccine plus celecoxib group compared with the vaccine plus celecoxib plus chemotherapy group ($p = 0.9$). Detailed p values comparing all groups are provided in Fig. 1*C*.

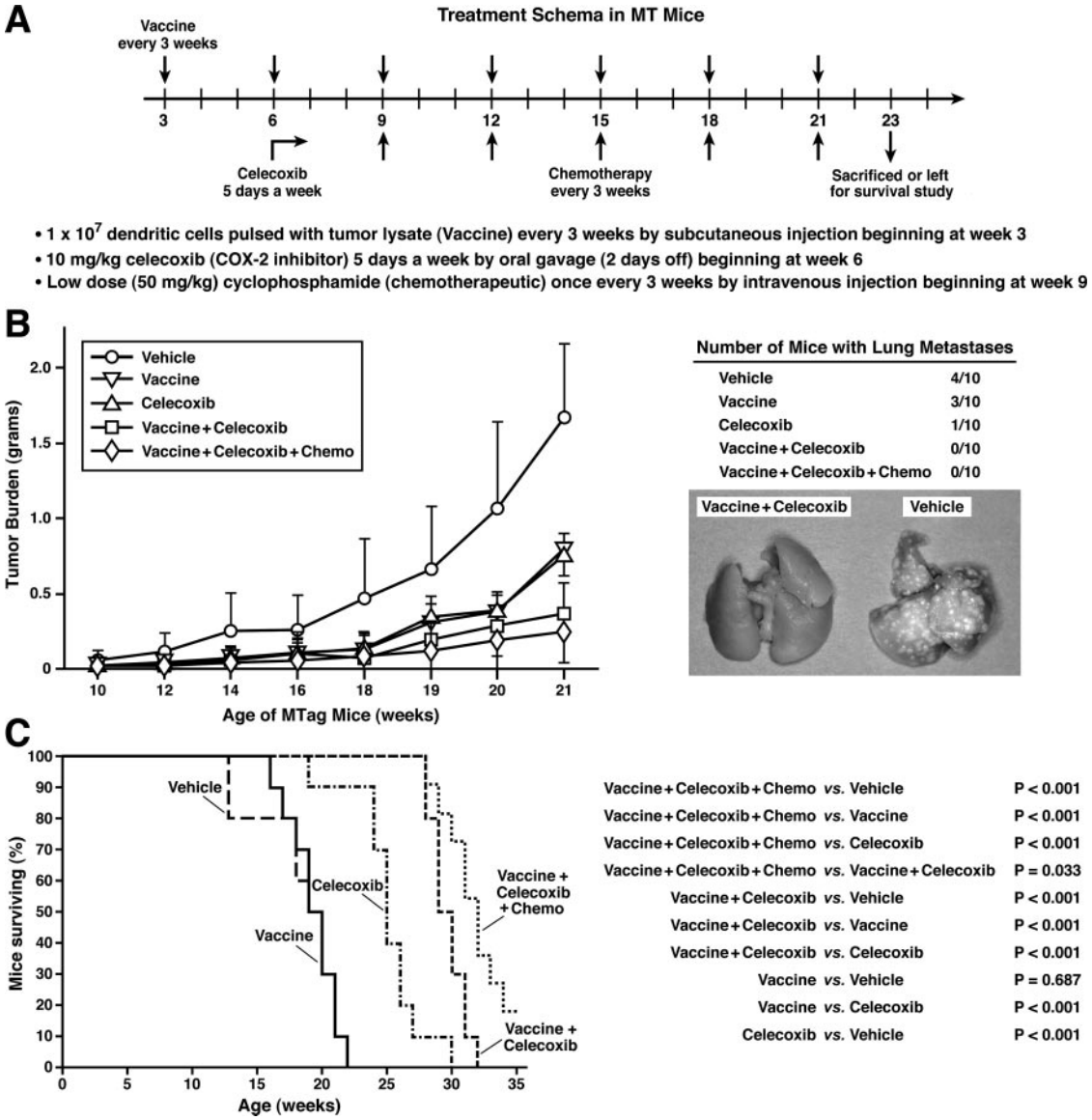

FIGURE 1. *A*, Schematic representation of the treatment schedule and dose in the PyV MT mice. *B*, Enhanced inhibition of mammary tumor growth and metastasis in PyV MT mice treated with combination regimen. Tumors were measured using digital calipers, and final weight was calculated as follows: $(L \times W^2)/2$. $n = 10$ mice. The vehicle group had significantly larger tumor burden than the celecoxib and vaccine-alone groups ($p < 0.0001$, actual value given below in a table form). However, the difference in tumor burden was markedly enhanced when vaccine was combined with celecoxib or with celecoxib plus chemotherapy ($p = 0.0001$). The *inset* shows the number of mice that developed lung metastasis and a representative image of lungs from PyV MT mice that were untreated vs treated with vaccine plus celecoxib. *C*, Enhanced survival in mice treated with combination regimen. Kaplan-Meier analysis of $n = 10$ mice for five treatment groups. Compared with mice treated with vehicle, survival was significantly enhanced by celecoxib treatment ($p < 0.0001$). However, survival was significantly improved when celecoxib was combined with either vaccine ($p < 0.0001$ compared with celecoxib or vaccine alone) or vaccine and chemotherapy ($p < 0.0001$ compared with celecoxib or vaccine alone). Vaccine alone had no significant effect on survival.

For survival studies, 10 mice per group were sacrificed when tumors reached >10% of mouse body weight. Parallel to the tumor burden, survival was significantly enhanced in mice treated with celecoxib alone ($p < 0.0001$ compared with control), vaccine plus celecoxib ($p < 0.0001$ compared with control, vaccine alone, or celecoxib alone), and vaccine plus celecoxib plus chemotherapy ($p < 0.0001$ compared with control, vaccine alone, or celecoxib alone) (Fig. 1*C*). Vaccine alone had no effect on survival compared with control. Because adding chemotherapy to the treatment regimen did not significantly affect tumor burden or survival, we chose to report only on the following five groups: 1) DMSO vehicle (control), 2) vaccine, 3) celecoxib, 4) vaccine plus celecoxib, and 5) vaccine plus celecoxib plus chemotherapy. Statistical analysis of the data revealed that, although an additive effect (interaction, 0.46 g; $p = 0.005$) was observed for the tumor burden between single modality (celecoxib or vaccine) and the combination (vaccine plus celelcoxib); a highly synergistic effect was observed for survival (interaction, 4.9 wk; $p < 0.001$).

Treatment with celecoxib reduces circulating PGE_2 levels in vivo

COX-2-derived PGE_2 is the major PG produced by breast cancer cells, and may be required for the angiogenic switch leading to initiation and progression of mammary cancer in a MMTV-COX-2 transgenic mouse model (17). Production of secreted PGE_2 is an appropriate measure of COX-2 activity in the PyV MT mouse model (24); however, PGE_2 is unstable in vivo, making measurement of its metabolite necessary to provide a reliable estimate of

actual PGE_2 production. Thus, we measured PGEM (namely, 13,14-dihydro-15-keto-PGA_2) in sera from all treatment groups by ELISA. A significant reduction in serum PGEM compared with control (Fig. 2*A*) was observed in mice treated with celecoxib alone, vaccine plus celecoxib, and vaccine plus celecoxib plus chemotherapy (2900 pg/ml in control, vs <1500 pg/ml in celecoxib alone or vaccine plus celecoxib ($p < 0.05$), vs ~500 pg/ml in vaccine plus celecoxib plus chemotherapy ($p < 0.005$)). Serum PGEM levels in nontumor C57BL/6 mice was ~300–400 pg/ml (24). As expected, there was no significant difference in PGEM levels between control and vaccine alone groups (Fig. 2*A*), whereas chemotherapy alone produced no significant decrease from control (data not shown). A similar pattern of PGEM expression was observed in tumor lysates (data not shown). In addition, there was a corresponding decrease in COX-2 expression in the tumor lysates by Western blot analysis (Fig. 2*B*) or by IHC (Fig. 2*C*) from these mice. Representative Western blots of COX-2 protein from one tumor section or lysate per treatment group are shown, with β-actin serving as the loading control. Using the ImageJ program, densitometric analysis was performed. Compared with vehicle group, ~20% lower COX-2 expression was determined in the vaccine group, whereas ~45–50% reduction was detected in the celecoxib, vaccine plus celecoxib, and vaccine plus celecoxib plus chemo groups. Why there was a slight reduction in COX-2 levels with vaccine alone given that PGEM levels did not change is not clear at this time. The only logical explanation is that the relationship of COX-2 protein expression in the tumor and PGEM in the serum is not always linear. Data shown are representative of three independent experiments. The relationship between the PGEM and tumor weight scores was assessed by using the Spearman rank correlation coefficient with weighted κ coefficient. There was a moderate but significant correlation between the two scores ($r = 0.87$; 95% confidence interval (CI), 0.60–0.96; $p < 0.001$). The 95% CI shows that the correlation is unlikely to be <0.60.

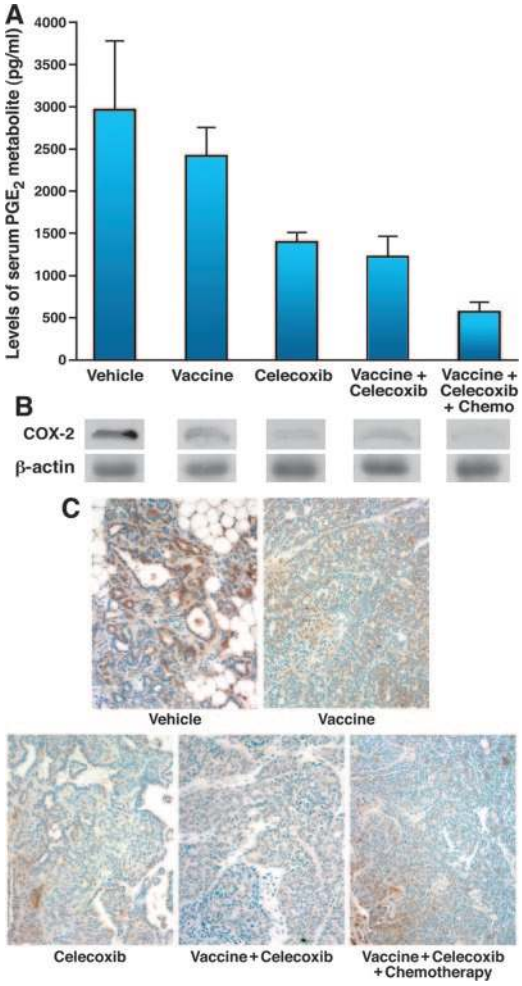

FIGURE 2. *A*, Inhibition of PGE_2 synthesis in serum of mice treated with celecoxib. Serum was collected from mice at time of sacrifice (~24 wk of age). PGEM levels in serum were determined using specific ELISA and values are shown as picograms/milliliter serum. Significant inhibition was observed in mice treated with celecoxib, and vaccine plus celecoxib ($p < 0.05$ compared with control or vaccine alone). Inhibition of PGEM in the serum was improved when chemotherapy was added to the treatment regimen ($p < 0.005$ compared with control; $p < 0.05$ compared with celecoxib alone). $n = 10$ mice per group. *B*, Reduced COX-2 expression with celecoxib treatment by Western blotting. Representative Western blot analysis showing COX-2 expression in tumor lysates from treated PyV MT mice. β-Actin Western was used as loading control. *C*, Reduced COX-2 expression with celecoxib treatment by IHC. Light microscopy image of COX-2 positivity. Mammary gland tumor sections (5 μm) from vehicle, celecoxib, vaccine, vaccine plus celecoxib, and vaccine plus celecoxib plus chemotherapy treated PyV MT mice. Brown staining represents COX-2 staining. All images are representative of five standardized fields from six separate mice. Images were taken at ×200 magnification.

Enhanced vaccine potency was associated with a significant increase in IFN-γ-producing $CD8^+$ CTLs and enhanced cytotoxicity

$CD4^+$ and $CD8^+$ T cells were sorted from TDLNs of treated and control mice and an IFN-γ-specific ELISPOT assay was performed. As expected, celecoxib alone did not cause any increase in IFN-γ-producing T cells compared with control, whereas vaccine alone caused ~15-fold increased IFN-γ spot formation in both $CD4^+$ and $CD8^+$ T cells ($p < 0.001$) (Fig. 3*A*). Interestingly, vaccine plus celecoxib significantly enhanced IFN-γ spot formation by $CD8^+$ T cells ($p < 0.01$, vs vaccine alone) suggesting a clear synergistic effect of vaccine plus celecoxib on antitumor IFN-γ response. This enhancement was not observed in the $CD4^+$ T cell population, suggesting a direct effect of vaccine plus celecoxib only on $CD8^+$ T cells. Importantly, addition of the suboptimal dose of chemotherapy to the treatment regimen did not reverse the beneficial effect of celecoxib on the antitumor IFN-γ response (Fig. 3*A*). To further examine the change in immunoregulatory cytokines in response to the different treatment groups, we conducted cytometric bead array assay on the T cell supernatants from the $CD4^+$ and $CD8^+$ T cells, which were used in the IFN-γ ELISPOT assay. The array of cytokines tested was TNF-α, IFN-γ, IL-12p, IL10, IL-6, and MCP-1. Of all the cytokines tested, TNF-α and IFN-γ were the only cytokines up-regulated with combination treatment as was seen in ELISPOT with IFN-γ. Secreted IL-10 was under the detection limit (data not shown).

The $CD8^+$ T cells were then tested for cytotoxicity. A standard 8-h ^{51}Cr release assay was conducted using PyV MT tumor cells as targets and TDLN-derived $CD8^+$ T cells as effectors. Vaccine alone elicited significantly higher lysis of target cells compared with control or celecoxib alone ($p < 0.01$) (Fig. 3*B*). Similar to the IFN-γ data, cytotoxicity of $CD8^+$ CTLs from the vaccine plus celecoxib group was 2-fold higher than with vaccine alone ($p < 0.01$), and 15-fold higher than control or celecoxib alone ($p < 0.001$). Again, addition of low-dose chemotherapy did not reverse the beneficial effect of celecoxib on the antitumor cytotoxic response (Fig. 3*B*). Statistical analysis of the percent lysis data revealed a clear synergy effect of vaccine plus celecoxib over single modality (interaction, 50% lysis; $p < 0.001$).

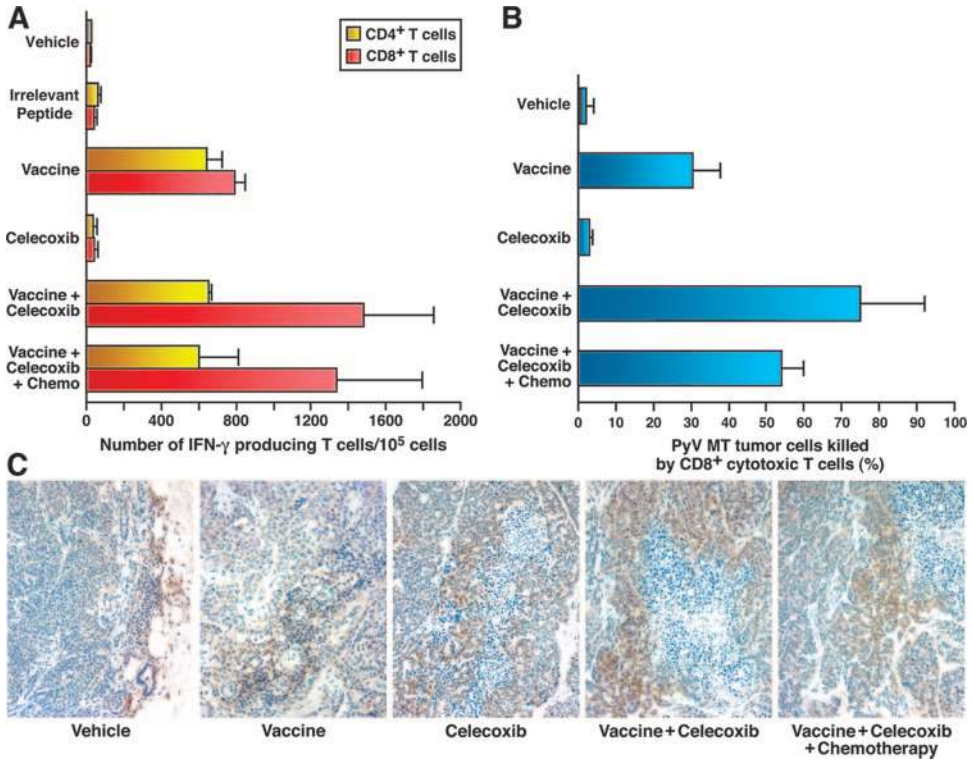

FIGURE 3. *A*, Celecoxib enhanced IFN-γ-producing $CD8^+$ T cells when administered in combination with DC vaccine. At sacrifice, $CD8^+$ and $CD4^+$ T cells were sorted from TDLNs. Cells were stimulated for 24 h with irradiated DCs pulsed with autologous tumor lysate, and IFN-γ-secreting T cells were evaluated by ELISPOT. Data are represented as spots per 10^5 T cells. Both $CD4^+$ and $CD8^+$ T cells showed increased IFN-γ spot formation in mice treated with vaccine compared with control mice (~15-fold increase; $p < 0.001$). Addition of celecoxib to the vaccine regimen significantly improved the IFN-γ spot formation specifically by $CD8^+$ T cells ($p < 0.01$ for vaccine vs vaccine plus celecoxib). Specificity of the assay was determined by stimulating T cells with DCs pulsed with irrelevant peptide. Addition of chemotherapy to the mix did not alter the response observed with vaccine plus celecoxib. $n = 10$ mice per group. *B*, Cytotoxicity of $CD8^+$ T cells against PyV MT tumor target cells is greatly enhanced in mice immunized with vaccine plus celecoxib. Effector cells from immunized mice were subjected to a standard ^{51}Cr release assay. PyV MT tumor cells were used as targets. Compared with control, a significant increase in CTL activity is observed with vaccine ($p < 0.01$), which was greatly enhanced in mice treated with a combination of vaccine plus celecoxib ($p < 0.001$ compared with control and $p < 0.01$ compared with vaccine alone). No cytotoxicity was observed with celecoxib alone. Addition of chemotherapy did not change the response observed in vaccine plus celecoxib group. $n = 10$ mice per group. No cytotoxicity was observed with a nonspecific tumor target (data not shown). *C*, Increased $CD8^+$ T cell infiltration in mice immunized with vaccine plus celecoxib with or without chemotherapy. Light microscopy images of $CD8^+$ T cells in mammary gland tumor sections (5 μm) from vehicle, celecoxib, vaccine, vaccine plus celecoxib, and vaccine plus celecoxib plus chemotherapy treated PyV MT mice. Note that infiltration is most evident around highly necrotic areas. In vehicle-treated mice, the $CD8^+$ T cells are in the periphery and are unable to enter the tumor bed. All images are representative of five standardized fields from six separate experiments. All images were taken at ×200 magnification.

Furthermore, we observed an increase in $CD8^+$ T cell infiltration in the tumor microenvironment with treatment, the highest infiltration being in the tumors treated with vaccine plus celecoxib with or without chemotherapy (Fig. 3*C*). Infiltration of the $CD8^+$ T cells is most evident around highly necrotic areas. In vehicle-treated mice, the $CD8^+$ T cells are in the periphery and are unable to enter the tumor bed. As expected, celecoxib and/or cyclophosphamide render the solid tumors leaky, and allow higher infiltration of the CTLs. In addition, due to reduced immunosuppressive COX-2/PGE_2 levels in the microenvironment, the CTLs are more likely to maintain their lytic activity. There were very few detectable $CD4^+$ T cells within the tumor (data not shown).

Expression of IDO was significantly reduced in response to combination treatment, coupled with increased PTEN and Bax, and decreased survivin

Lysates were prepared from tumors excised from mice sacrificed at age 21–23 wk. Western blot analysis of IDO clearly indicates decreased levels in tumor lysates from mice treated with celecoxib alone (Fig. 4*A*). This decrease was more pronounced in lysates from mice treated with the combination of vaccine plus celecoxib, or vaccine plus celecoxib plus chemotherapy. IHC of the tumor sections confirms the Western blot data with highest expression of IDO expression in the vehicle treatment and lowest in the vaccine plus celecoxib with or without cyclophosphamide (Fig. 4*C*). Chemotherapy alone had no effect (data not shown). In addition, the combination therapies of vaccine plus celecoxib and vaccine plus celecoxib plus chemotherapy demonstrate increased expression of the PTEN tumor suppressor and Bax, a proapoptotic protein, along with reduced expression of survivin, an antiapoptotic protein (Fig. 3*A*). Western blots of tumor lysates from three individual mice are shown, with β-actin to show equal loading of the samples. Densitometric analysis was conducted using the ImageJ program. The data are shown in a histogram in Fig. 4*B*. Detailed statistics for the densitometry data is provided in Table I. All treatment groups showed significant decrease in IDO levels compared with vehicle treatment, nevertheless, the difference between vaccine or celecoxib alone and vaccine plus celecoxib plus cyclophosphamide was significant ($p < 0.001$ and $p \leq 0.03$, respectively). Although a trend toward decrease is noticed in the survivin protein (antiapoptotic) levels, the only significant difference was observed between the vehicle and the vaccine plus celecoxib plus

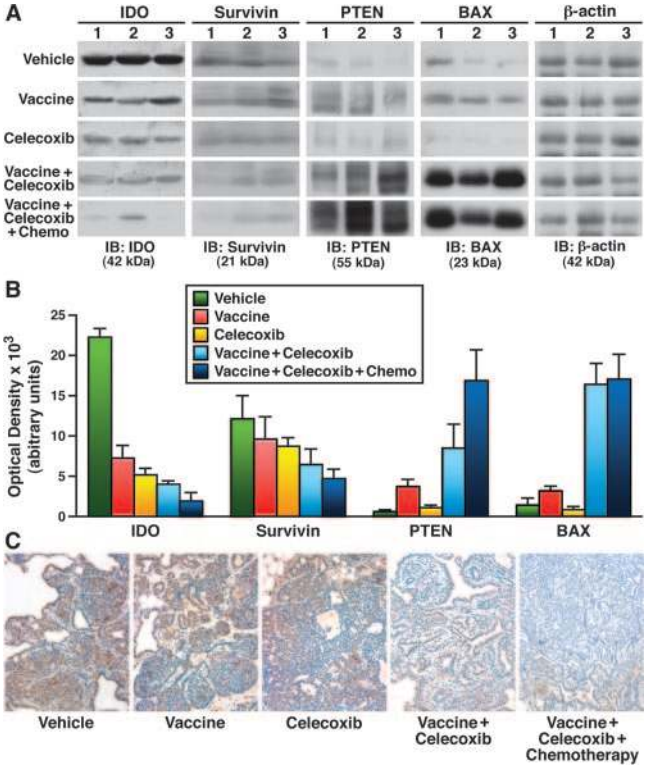

FIGURE 4. Enhanced tumor reduction and enhanced antitumor immune response in PyV MT mice treated with combination treatment were associated with decreased IDO and survivin; and increased PTEN and Bax proteins. *A*, Western blot analysis. Tumors were collected at time of sacrifice (23 wk of age) and Western blot analysis of tumor lysate was conducted from control and treated mice as indicated. Three individual mouse data are shown. A total of 100 μg of lysate was added per lane. β-Actin Ab was used as loading control. Western blots were repeated three times with similar results. Decrease in IDO protein levels is observed with single modality (vaccine or celecoxib). This decrease is significantly enhanced with the combination of the vaccine plus celecoxib or when combined with chemotherapy. *B*, Densitometric analysis of the above Western blots. Graphic representation of the densitometric analysis. ImageJ program was used to generate the data. Significant differences were observed between single modality and combination treatment. Statistical significance is tabulated in Table I. *C*, IDO expression is decreased with combination treatment. Light microscopy images of IDO expression in mammary gland tumor sections (5 μm) from treated PyV MT mice. Brown stain represents IDO staining. These data confirm the Western blot data where decrease in IDO expression is enhanced when mice are treated with the combination compared with a single agent. All images are representative of five standardized fields from six separate experiments. All images were taken at $\times$200 magnification.

cyclophosphamide group. In contrast, significant increase in bax protein (proapoptotic) is observed between vehicle, vaccine, or celecoxib alone treated groups vs vaccine plus celecoxib with or without cyclophosphamide group ($p < 0.001$). Similar to bax protein, there is significant increase in PTEN tumor suppressor protein, in the vaccine plus celelcoxib with or without cyclophosphamide treated groups compared with vehicle, vaccine, or celecoxib alone ($p < 0.001$). Interestingly, there is significant difference between vaccine plus celecoxib vs vaccine plus celecoxib plus cyclophosphamide ($p = 0.02$). Data indicate that the combination treatment 1) enhances CTL function by decreasing expression of IDO (a potent suppressor of T cell function), 2) enhances in situ apoptosis by increasing expression of the proapoptotic protein bax, and 3) decreases in situ proliferation by increasing expression of tumor suppressor protein PTEN.

Table I. *Statistical significance (*p *values) of the densitometry data for IDO, survivin, PTEN, and Bax proteins*[a]

	P
IDO	
Vaccine + celecoxib + chemo vs vehicle	$1.17e\times10^{-9}$
Vaccine + celecoxib + chemo vs celecoxib	0.002
Vaccine + celecoxib + chemo vs vaccine	0.00001
Vaccine + celecoxib + chemo vs vaccine + celecoxib	0.11
Vaccine + celecoxib vs vehicle	$2.8e\times10^{-9}$
Vaccine + celecoxib vs celecoxib	0.03
Vaccine + celecoxib vs vaccine	0.01
Celecoxib vs vehicle	$9.4e\times10^{-9}$
Celecoxib vs vaccine	0.005
Vaccine vs vehicle	$8.8e\times10^{-8}$
Survivin	
Vaccine + celecoxib + chemo vs vehicle	0.02
Vaccine + celecoxib + chemo vs celecoxib	0.1
Vaccine + celecoxib + chemo vs vaccine	0.2
Vaccine + celecoxib + chemo vs vaccine + celecoxib	0.5
Vaccine + celecoxib vs vehicle	0.05
Vaccine + celecoxib vs celecoxib	0.3
Vaccine + celecoxib vs vaccine	0.4
Celecoxib vs vehicle	0.4
Celecoxib vs vaccine	0.7
Vaccine vs vehicle	0.2
PTEN	
Vaccine + celecoxib + chemo vs vehicle	0.0003
Vaccine + celecoxib + chemo vs celecoxib	0.0004
Vaccine + celecoxib + chemo vs vaccine	0.001
Vaccine + celecoxib + chemo vs vaccine + celecoxib	0.02
Vaccine + celecoxib vs vehicle	0.02
Vaccine + celecoxib vs celecoxib	0.03
Vaccine + celecoxib vs vaccine	0.05
Celecoxib vs vehicle	0.8
Celecoxib vs vaccine	0.4
Vaccine vs vehicle	0.3
Bax	
Vaccine + celecoxib + chemo vs vehicle	0.0001
Vaccine + celecoxib + chemo vs celecoxib	0.00009
Vaccine + celecoxib + chemo vs vaccine	0.0003
Vaccine + celecoxib + chemo vs vaccine + celecoxib	0.8
Vaccine + celecoxib vs vehicle	0.0001
Vaccine + celecoxib vs celecoxib	0.0001
Vaccine + celecoxib vs vaccine	0.0004
Celecoxib vs vehicle	0.05
Celecoxib vs vaccine	0.3
Vaccine vs vehicle	0.5

[a] Densitometric analysis was conducted using the ImageJ program and is presented in Fig. 4B.

Apoptosis was increased and proliferation was decreased in tumor cells treated with combination therapy

For direct evidence of apoptosis in the tumors, primary PyV MT tumor cells were stained with annexin V and PI for analysis by flow cytometry (24). Apoptotic cells were defined as those that were positive for both stains. We confirmed that, compared with control, there was significant (~3-fold) increase in the apoptotic cell population in tumors from the celecoxib alone or vaccine alone groups (Table II, 7% in control vs 29% in celecoxib alone and 23% in vaccine alone (both $p < 0.05$)). However, in the combination treatments, with or without chemotherapy, the apoptotic population was significantly ($p < 0.05$) enhanced compared with vaccine alone or celecoxib alone groups (Table II, 42% in vaccine plus celecoxib, and 55% in vaccine plus celecoxib plus chemotherapy vs 23% in vaccine alone or 29% in celecoxib alone). Compared with control, both combination treatments showed a

Table II. *Enhanced apoptosis of PyV MT tumor cells in vivo in mice treated with combination therapy*[a]

Treatment Groups	Percent Apoptotic Cells (annexin $V^+/P1^+$)	p Value Compared with Control	p Value Compared with Celecoxib	p Value Compared with Vaccine
Vehicle	7 ± 3		$p < 0.05$	$p < 0.05$
Vaccine	23 ± 10	$p < 0.05$	NS	
Celecoxib	29 ± 12	$p < 0.05$		NS
Vaccine + celecoxib	42 ± 11	$p < 0.001$	$p < 0.05$	$p < 0.05$
Vaccine + celecoxib + chemotherapy	55 ± 15	$p < 0.001$	$p < 0.05$	$p < 0.05$

[a] Apoptosis of primary PyV MT tumor cells was determined by annexin V/PI staining. Compared with mice treated with vehicle, there was significant increase in apoptotic cell population in tumors of mice treated with celecoxib alone or vaccine alone ($p < 0.05$). However, the apoptotic population was significantly enhanced when celecoxib was combined with vaccine and/or chemotherapy ($p < 0.001$ compared with control; and $p < 0.05$ compared with vaccine or celecoxib alone).

significant increase in the apoptotic population ($p < 0.001$). Flow cytometry data were confirmed using in situ TUNEL staining of tumor sections from all treatment groups. Mice treated with vaccine plus celecoxib or vaccine plus celecoxib plus chemotherapy show significantly higher TUNEL-positive cells than tumors from mice treated with vehicle, celecoxib alone, or vaccine alone (Fig. 5*A*). Enhanced PTEN expression should correlate with lower proliferation of the tumor cell. PCNA staining pattern clearly show reduced PCNA staining (suggestive of reduced proliferating cells) in tumor sections dissected from mice treated with the combination compared with tumors from mice treated with vehicle, vaccine, or celecoxib alone (Fig. 5*B*). Decrease in proliferation and increase in apoptosis in situ within the tumor correlated with lower tumor burden and increased survival (Fig. 1, *B* and *C*).

Low-level expression of IDO protein in DCs isolated from tumor-bearing PyV MT mice

IFN-γ production is known to have immunoregulatory activities and it has been shown to induce IDO in some cultured cells including tumor cells and APCs. Because we observe high IFN-γ production by T cells, we determined the level of IDO in the DCs isolated from bone marrow or lymph nodes of 18-wk-old tumor-bearing PyV MT mice by Western blot analysis. IDO expression was as low as that observed in DCs isolated from non-tumor-bearing C57BL/6 WT mice (Fig. 6*A*). There was no significant difference between immature DCs and DCs matured with LPS (Fig. 6*A*). IDO expression remained unchanged when DCs were pulsed with PyV MT tumor lysate (data not shown). Whether DCs were derived from the bone marrow, lymph node, or spleen did not make a difference (data not shown). Fig. 6*A* shows IDO expression from bone marrow-derived DCs. Furthermore, we observed no significant difference in DC phenotype (as measured by expression of IDO, CD11c, B7.1, B7.2, CD40, B7H1, or MHC class I or II) between WT C57BL/6, vehicle-treated, or vaccine- plus celecoxib-treated PyV MT mice (data not shown). IDO expression was most profound in the tumor itself suggesting that the IDO-related effects in the PyV MT mice is primarily associated with the tumor itself rather than with the lymphoid organs. Therefore, further analysis of DCs from treated mice was not pursued.

IDO expression is low in the PyV MT-derived tumor cell lines

Because PyV MT cell lines were used as targets in the ^{51}Cr release CTL assay, it is conceivable that the CTLs incubated on these targets could be adversely affected. Although CTL data does not suggest this to be the case (Fig. 3), we examined the levels of IDO in these cell lines by Western blotting and IHC. Compared with the

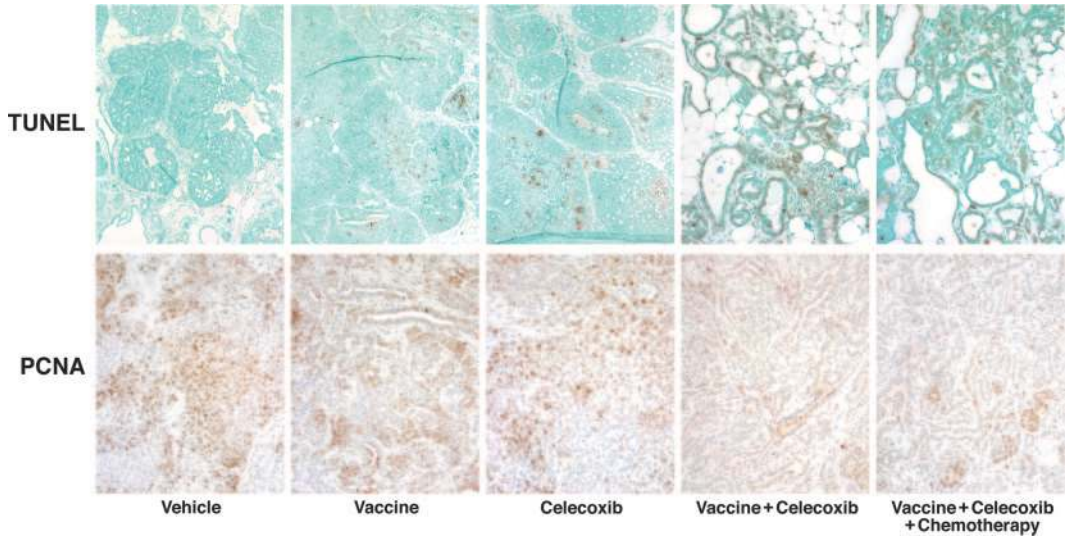

FIGURE 5. *A*, Increase in TUNEL-positive cells with combination treatment in PyV MT tumors in situ. Light microscopy image of TUNEL-positive cells to visualize apoptosis in situ in mammary gland tumor sections (5 μm) from treated PyV MT mice. Brown staining represents apoptotic cells. Highest TUNEL positivity is observed in tumors section from mice treated with vaccine plus celecoxib or vaccine plus celecoxib plus chemotherapy. All images are representative of five standardized fields from six separate mice. Images were taken at ×200 magnification. *B*, Combination treatment induced inhibition of tumor cell proliferation in vivo. Light microscopy images of PCNA staining of 5-μm mammary tumor sections from treated PyV MT mice. Brown staining represents PCNA staining. All images are representative of five standardized fields from six separate experiments. Inhibition of proliferation is most evident with vaccine plus celecoxib or vaccine plus celecoxib plus chemotherapy. All images were taken at ×200 magnification.

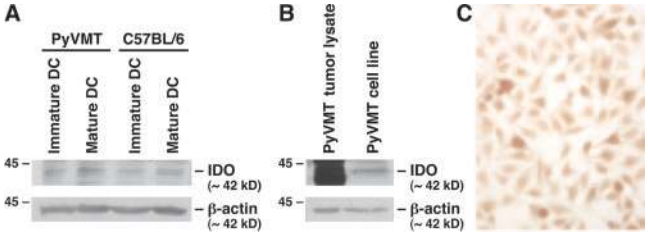

FIGURE 6. *A*, Low IDO protein expression in DCs isolated from tumor-bearing PyV MT mice. Bone marrow-derived DCs were prepared from PyV MT and C57BL/6 mice at 18 wk of age, and Western blot analysis was performed on immature and mature DCs. DCs were matured using 1 μg/ml LPS. A total of 100 μg of lysate was added per lane. β-Actin Ab was used as loading control. Western blots were repeated three times with similar results. Levels of IDO from tumor-bearing PyV MT and nontumor-bearing C57BL/6 mice were similar, and maturing with LPS did not substantially alter the levels. *B*, Compared with PyV MT primary tumor lysate, the PyV MT tumor cell lines express significantly lower levels of IDO. Western blot analysis of lysates prepared from primary tumor and cell lines is shown. A total of 100 μg of lysate was added per lane. β-Actin Ab was used as loading control. Western blots were repeated three times with similar results. *C*, Homogeneous expression of IDO in the PyV MT cell lines. Cell lines were grown in chamber slides. Before staining, cells were permeabilized, fixed, and stained for IDO expression. All cells express IDO. Staining was repeated three times with similar results. Image was taken at $\times$100 magnification.

primary tumor lysate, IDO expression is low in the PyV MT-derived tumor cell lines (Fig. 6, *B* and *C*). This confirms that the target cells used in our study were appropriate and that these tumor cells were unable to induce IDO-associated T cell suppression.

IDO expression decreases with COX-2 down-regulation in MDA-MB-231 human breast cancer cells

To verify our in vivo observation that inhibition of COX-2 was associated with decreased IDO expression, we examined IDO levels after down-regulating COX-2 using siRNA in a human breast cancer cell line, MDA-MB-231. Ideally, this experiment should have been conducted in the PyV MT cell lines; however, we were unable to transfect these cell lines. Five transfection reagents and various transfection protocols were used with limited success. Therefore, we selected a cell line that is known to express both COX-2 and IDO abundantly and are highly metastatic in nature (47, 48). Significant knock-down of COX-2 protein level was achieved in the MDA-MB-231 cells with COX-2-specific siRNA (50 nM) (Fig. 7*A*). Associated with COX-2 down-regulation, we observed a significant knock-down of IDO expression, confirming the in vivo data that inhibiting COX-2 with celecoxib can regulate expression of IDO in the PyV MT primary tumor. Supplementation of PGE_2 to the COX-2-depleted cells restored IDO expression (data not shown).

A positive correlation exists between expression of COX-2 and IDO in primary human breast cancer specimens

To correlate our preclinical studies with human disease, we stained a panel of 15 human breast cancer specimens of different grades for COX-2 and IDO levels. High-grade invasive tumor specimens (Nottingham grade 3/3) were found to express high COX-2 with correspondingly high IDO in equivalent areas of the tumor, whereas low-grade tumors (Nottingham grade 2/3) had low COX-2 corresponding with low IDO expression (Table III). The relationship between the COX2 and IDO scores was assessed by using the Spearman rank correlation coefficient and weighted κ coefficient. There was a strong correlation between the two scores

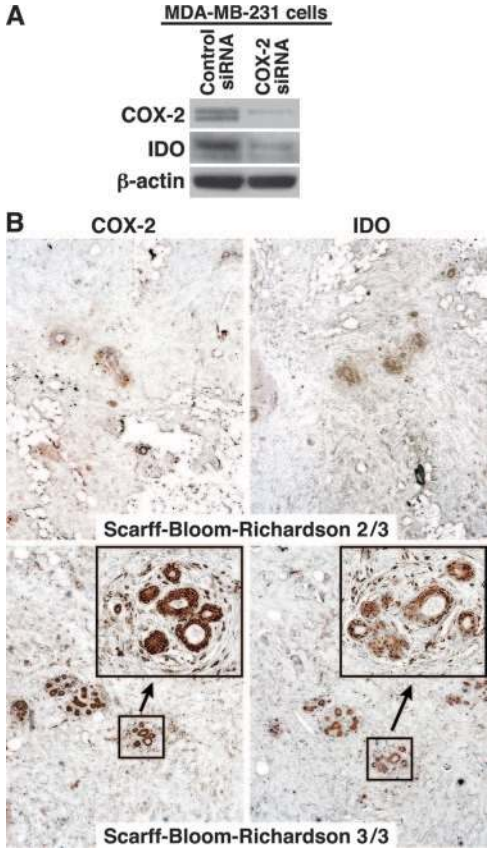

FIGURE 7. *A*, IDO expression decreases when COX-2 is knocked down in MDA-MB-231 breast cancer cells. Expression of COX-2 and IDO in MDA-MB-231 cells was measured by Western blot. Treatment with a COX-2 siRNA for 48 h significantly inhibited COX-2 expression at siRNA concentrations of 50 nM, with a subsequent decrease in expression of IDO protein. Data shown are representative of three independent experiments. *B*, Expression of COX-2 and IDO in primary human breast cancer tissue. Representative immunohistochemical staining showing COX-2 and IDO expression in primary human grade 3 and grade 2 breast tumor specimens. Images were taken at $\times$100 magnification. *Inset* shows greater magnification ($\times$200).

(r = 0.99; 95% CI, 0.98–1.00). The 95% CI shows that the correlation is unlikely to be <0.98. Due to low sample size, significant correlation between tumor grade and COX-2/IDO staining intensity was not reached. Representative COX-2 and IDO staining patterns for high-grade metastatic and low-grade nonmetastatic ductal carcinomas are shown (Fig. 7*B*). We have previously analyzed the PBMCs from the same human patients (from which the tumor tissues were procured for this paper) for their T cell and DC function and compared it to age-matched normals. Patients with high COX-2 and PGE_2 expression were found to have significantly lower T cell and DC function (12). We then analyzed the IDO expression on the same individuals for this study and found a direct correlation with COX-2 expression. Thus, we believe that this finding is immunologically significant and may help not only in designing novel immunotherapeutic strategies for patients with metastatic breast cancer but also in selecting the patients that may most benefit from such therapies.

Discussion

These results clearly suggest that combining celecoxib with a DC-based tumor vaccine increased the vaccine efficacy by severalfold compared with either treatment alone. Mice treated with combination therapy developed highly lytic, long-lasting CTLs that were

Table III. *Positive correlation between COX-2 and IDO staining intensity in primary breast cancer specimens*[a]

Patient No. (Stage of Cancer)	COX-2 Staining Intensity	IDO Staining Intensity
1 Stage 1	++	+
2 Stage 3 (LN+)	+++	++
3 Stage 1	++	+
4 Stage 2	+++	++
5 Stage 3 (LN+)	++++	+++
6 Stage 2	+++	++
7 Stage 2	+++	++
8 Stage 2	+++	++
9 Stage 1	+++	++
10 Stage 3	+++	++
11 Stage 1	+	+
12 Stage 2 (LN+)	+++	+++
13 Stage 1	++	+
14 Stage 3 (LN+)	++++	+++
15 Stage 2	+++	++

[a] All patient specimens were from infiltrating ductal lobular carcinoma of the breast ranging from Scarff-Bloom-Richardson grades 1/3 ($n = 5$), grade 2/3 ($n = 6$), and grade 3/3 ($n = 4$). Of these, four were lymph node positive as indicated (LN+). Staining intensity was determined by immunohistochemistry. Staining intensity was recorded on a scale of + to ++++, with + being low intensity and ++++ being high intensity. The relationship between the COX2 and IDO scores was assessed by using the Spearman rank correlation coefficient. There was a strong correlation between the two scores ($r = 0.99$, 95% CI, 0.98–1.00). The 95% CI shows that the correlation is unlikely to be <0.98.

significantly more effective than CTLs from control, vaccine alone, or celecoxib alone groups. The enhanced CTL activity associated with decreased PGEM and COX-2 levels translated well to clinical response, with significant reduction in primary tumors, complete eradication of lung metastases, and increased survival. Given the extremely powerful nature of the PyV MT oncogene, the 2- to 3-fold increase in survival represents a remarkable success in treatment of these tumors. Importantly, low-dose chemotherapy did not diminish the synergistic activation of CTLs seen with vaccine plus celecoxib treatment, suggesting that combination of all three therapies may be a feasible means of reducing toxicity to patients without reducing treatment efficacy.

There was a ~2-fold increase in the apoptotic population of tumor cells when vaccine was combined with celecoxib or celecoxib plus chemotherapy compared with vaccine alone or celecoxib alone. The proapoptotic protein Bax was greatly elevated in the treated tumors, accompanied by decrease of the antiapoptotic protein survivin. In addition, levels of PTEN, a tumor suppressor that regulates cell survival through the PI3K pathway, were significantly enhanced in the treated vs control animals. PTEN, a lipid phosphatase, is the most important negative regulator of the cell survival signaling pathway initiated by the PI3K signaling pathway (49). The PI3K pathway is an important driver of cell proliferation and cell survival. When PTEN is inactivated, activation of PI3K effectors—particularly the activation of key survival kinase PKB (also known as Akt) can occur in the absence of any exogenous stimulus, and tumorigenesis occurs. Activation of PKB/Akt is directly associated with decreased activation of proapoptotic proteins including Bax (49). Thus, reactivation of PTEN with the combination treatment may lead to the inactivation of PI3K/Akt and activation of downstream Bax protein (Fig. 4). Inactivation of PI3K/Akt as the mechanism of celecoxib-induced tumor cell apoptosis has previously been noted in our laboratory as well as by others (24, 50, 51). In the PyV MT mice, mammary gland tumors are induced by the action of a potent tyrosine kinase activity associated with the polyoma virus middle T Ag driven by the mouse mammary tumor virus long terminal repeat (MMTV) (40). Therefore, it is striking that the inactivation of PTEN in these tumors is reversed in the mice that are treated with the combination but not with the single agents. We would like to believe that the CTLs that were significantly more lytic and that infiltrated the tumors of mice treated with the combination are partly responsible for the high apoptosis with corresponding high Bax expression, and low proliferation with corresponding high PTEN expression. Infiltration of the $CD8^+$ T cells is most evident around highly necrotic areas (Fig. 3*C*). In vehicle-treated mice, the $CD8^+$ T cells are in the periphery and are unable to enter the tumor bed (Fig. 3*C*). In the vaccine-treated mice, although we observe high CTL activity in vitro (Fig. 3*B*), the $CD8^+$ T cell infiltration is minimal. This could explain why Bax and PTEN have not changed in vaccine-treated mice. As is expected, celecoxib and/or cyclophosphamide render the solid tumors leaky, and allow higher infiltration of the CTLs (Fig. 3*C*). These results suggest that the combination treatments target the apoptotic/survival pathway and may have great potential for reduction of primary tumors as well as prevention of metastatic spread, and contribute to the observed survival benefit.

As IDO catalyzes tryptophan degradation and inhibits T cell proliferation within the tumor microenvironment, our results suggest that enhanced CTL activity after combination treatment may be due in part to the decrease in tumor IDO levels. Originally identified in the placenta, IDO has recently been detected in many cancers including breast cancer, where it has been implicated in immune escape (25, 26, 39). A mechanistic link was demonstrated between IDO and the tolerance-inducing activity of CTLA4-Ig, whereby binding of CTLA4-Ig to B7-1 and B7-2 receptors on the surface of DCs activated a signaling pathway leading to the induction of IDO (52). Expression of IDO has been observed in cells exposed to PGE_2 or IFN-γ and in certain types of activated macrophages and tolerizing DCs (29, 30, 38, 53, 54). In our model, increased IFN-γ secretion by T cells in the periphery (i.e., the TDLN) (Fig. 3, *A* and *B*) did not change the IDO levels in the DCs derived from the same mice (data not shown). Given that the IDO expression in PyV MT-derived DCs was minimal (Fig. 6*A*), we do not expect to observe a tolerizing effect of the lymphoid DCs from the PyV MT mice on the T cells. In fact, the importance of IFN-γ in enhancing tumor immunogenicity in vivo has been shown repeatedly, at least in part, due to increased MHC class I pathway activity in the tumor targets leading to their more effective recognition by $CD8^+$ T cells (10, 55–58). Although we did not test IFN-γ levels in the tumor microenvironment, we did test the COX-2 expression (Fig. 2, *B* and *C*) because COX-2-derived PGE_2 is a potent inducer of IDO. Data clearly suggest that the IDO levels correlated with the depletion of COX-2/PGE_2 (Figs. 2, 4, and 7). PGE_2 is a potent T cell suppressor; however, the mechanism by which PGE_2 renders its immunosuppressive effect is not clear. Because PGE_2 is a known inducer of IDO expression in APCs (59, 60), it is conceivable that high PGE_2 in the tumor environment may induce IDO expression. Thus, inhibiting COX-2/PGE_2 specifically reduces IDO expression in vivo (Fig. 4) and in vitro (Fig. 7). Our preclinical studies offer us an opportunity to assess the feasibility of inhibition of IDO in combination with immunotherapy and low-dose chemotherapy for the treatment of breast cancer and/or prevention of metastatic spread. This is especially relevant at a time when clinical trials with COX-2 inhibitors are under debate and safer alternative agents are desired.

To correlate our in vivo preclinical studies with human disease, we first show that modulating COX-2 in the highly metastatic MDA-MB-231 breast cancer cell line has a direct effect on IDO expression. IDO expression decreases with depletion of COX-2 and increases upon supplementation with PGE_2. It is known that the highly aggressive MDA-MB-231 cells express high levels of

IDO and COX-2, whereas the nonaggressive, nonmetastatic MCF-7 breast cancer cells have low COX-2 and correspondingly low IDO expression (47, 48, 61), indicating a likely association between the activity of these two enzymes and the aggressiveness of breast cancer cell lines. Second, we show a direct correlation between COX-2 and IDO expression in primary human breast cancer specimens. We also observed higher COX-2 and IDO expression in high-grade tumor specimens, although the sample size was too small for statistical significance. In primary human breast cancer, elevated COX-2 expression has been previously associated with large tumor size and high histological grade in breast cancer (62). No such association, although one likely exists, has yet been established for IDO.

The ability of effector CTLs to compete with a growing tumor and the immunosuppressive factors it releases is a crucial factor in the success of a cancer vaccine. In addition to demonstrating a novel link between COX-2 expression and the level of IDO in human breast cancer, our results indicate that the combination treatment of a DC-based vaccine plus celecoxib enhanced CTL activity, decreased activity of the COX-2 pathway in tumor cells, activated tumor cell apoptosis by activating Bax and PTEN, and resulted in increased survival and abrogation of metastasis. These preclinical data are supported by a clear link between COX-2 and IDO in human breast cancer, suggesting that inhibition of COX-2 in combination with immunotherapy has great potential in the treatment of primary tumors as well as in the prevention of metastatic spread.

Acknowledgments

We acknowledge Dr. Sandra J. Gendler for her helpful scientific suggestions and for critical review of the article. We thank Brie Noble, and Dr. Joseph Hentz in the Biostaistics core for help with statistical analysis. We thank Latha B. Pathangey and Michelle L. Owens for their technical help. We also acknowledge all technicians in the Natalie Schaffer transgenic animal facility and in the histology core; Marvin Ruona in the visual communications core for his expertise in preparation of the figures; and Irene Beauvais for help in submitting the manuscript.

Disclosures

The authors have no financial conflict of interest.

References

1. Mukherjee, P., A. R. Ginardi, C. S. Madsen, T. L. Tinder, F. Jacobs, J. Parker, B. Agrawal, B. M. Longenecker, and S. J. Gendler. 2001. MUC1-specific CTLs are non-functional within a pancreatic tumor microenvironment. *Glycoconj. J.* 18: 931–942.
2. Mukherjee, P., T. L. Tinder, G. D. Basu, L. B. Pathangey, L. Chen, and S. J. Gendler. 2004. Therapeutic efficacy of MUC1-specific cytotoxic T lymphocytes and CD137 co-stimulation in a spontaneous breast cancer model. *Breast Dis.* 20: 53–63.
3. Laheru, D., B. Biedrzycki, and E. M. Jaffee. 2001. Immunologic approaches to the management of pancreatic cancer. *Cancer J.* 7: 324–337.
4. Simons, J. W., E. M. Jaffee, C. E. Weber, H. I. Levitsky, W. G. Nelson, M. A. Carducci, A. J. Lazenby, L. K. Cohen, C. C. Finn, S. M. Clift, et al. 1997. Bioactivity of autologous irradiated renal cell carcinoma vaccines generated by ex vivo granulocyte-macrophage colony-stimulating factor gene transfer. *Cancer Res.* 57: 1537–1546.
5. Soiffer, R., T. Lynch, M. Mihm, K. Jung, C. Rhuda, J. C. Schmollinger, F. S. Hodi, L. Liebster, P. Lam, S. Mentzer, et al. 1998. Vaccination with irradiated autologous melanoma cells engineered to secrete human granulocyte-macrophage colony-stimulating factor generates potent antitumor immunity in patients with metastatic melanoma. *Proc. Natl. Acad. Sci. USA* 95: 13141–13146.
6. Jaffee, E. M., R. Abrams, J. Cameron, R. Donehower, M. Duerr, J. Gossett, T. F. Greten, L. Grochow, R. Hruban, S. Kern, et al. 1998. A phase I clinical trial of lethally irradiated allogeneic pancreatic tumor cells transfected with the GM-CSF gene for the treatment of pancreatic adenocarcinoma. *Hum. Gene Ther.* 9: 1951–1971.
7. Simons, J. W., B. Mikhak, J. F. Chang, A. M. DeMarzo, M. A. Carducci, M. Lim, C. E. Weber, A. A. Baccala, M. A. Goemann, S. M. Clift, et al. 1999. Induction of immunity to prostate cancer antigens: results of a clinical trial of vaccination with irradiated autologous prostate tumor cells engineered to secrete granulocyte-macrophage colony-stimulating factor using ex vivo gene transfer. *Cancer Res.* 59: 5160–5168.
8. Mukherjee, P., A. R. Ginardi, C. S. Madsen, C. J. Sterner, M. C. Adriance, M. J. Tevethia, and S. J. Gendler. 2000. Mice with spontaneous pancreatic cancer naturally develop MUC1-specific CTLs that eradicate tumors when adoptively transferred. *J. Immunol.* 165: 3451–3460.
9. Mukherjee, P., A. R. Ginardi, T. L. Tinder, C. J. Sterner, and S. J. Gendler. 2001. MUC1-specific CTLs eradicate tumors when adoptively transferred in vivo. *Clin. Can. Res.* 7: 848s–855s.
10. Mukherjee, P., C. S. Madsen, A. R. Ginardi, T. L. Tinder, F. Jacobs, J. Parker, B. Agrawal, B. M. Longenecker, and S. J. Gendler. 2003. Mucin 1-specific immunotherapy in a mouse model of spontaneous breast cancer. *J. Immunother.* 26: 47–62.
11. Mukherjee, P. G. A., C. S. Madsen, T. L. Tinder, F. Jacobs, J. Parker, B. Agrawal, B. M. Longenecker, and S. J. Gendler. 2003. MUC1-specific CTLs are non-functional within a pancreatic tumor microenvironment. *Glycoconj. J.* 18: 931–942.
12. Pockaj, B. A., G. D. Basu, L. B. Pathangey, R. J. Gray, J. L. Hernandez, S. J. Gendler, and P. Mukherjee. 2004. Reduced T-cell and dendritic cell function is related to cyclooxygenase-2 overexpression and prostaglandin E_2 secretion in patients with breast cancer. *Ann. Surg. Oncol.* 11: 328–339.
13. Zha, S., V. Yegnasubramanian, W. G. Nelson, W. B. Isaacs, and A. M. De Marzo. 2004. Cyclooxygenases in cancer: progress and perspective. *Cancer Lett.* 215: 1–20.
14. Dannenberg, A. J., and K. Subbaramaiah. 2003. Targeting cyclooxygenase-2 in human neoplasia: rationale and promise. *Cancer Cell* 4: 431–436.
15. Okuno, K., H. Jinnai, Y. S. Lee, K. Nakamura, T. Hirohata, H. Shigeoka, and M. Yasutomi. 1995. A high level of prostaglandin E_2 (PGE_2) in the portal vein suppresses liver-associated immunity and promotes liver metastases. *Surg. Today* 25: 954–958.
16. Takayama, K., G. Garcia-Cardena, G. K. Sukhova, J. Comander, M. A. Gimbrone, Jr., and P. Libby. 2002. Prostaglandin E_2 suppresses chemokine production in human macrophages through the EP4 receptor. *J. Biol. Chem.* 277: 44147–44154.
17. Chang, S. H., C. H. Liu, R. Conway, D. K. Han, K. Nithipatikom, O. C. Trifan, T. F. Lane, and T. Hla. 2004. Role of prostaglandin E_2-dependent angiogenic switch in cyclooxygenase 2-induced breast cancer progression. *Proc. Natl. Acad. Sci. USA* 101: 591–596.
18. Harizi, H., C. Grosset, and N. Gualde. 2003. Prostaglandin E_2 modulates dendritic cell function via EP2 and EP4 receptor subtypes. *J. Leukocyte Biol.* 73: 756–763.
19. Morecki, S., E. Yacovlev, Y. Gelfand, V. Trembovler, E. Shohami, and S. Slavin. 2000. Induction of antitumor immunity by indomethacin. *Cancer Immunol. Immunother.* 48: 613–620.
20. Chang, S. H., Y. Ai, R. M. Breyer, T. F. Lane, and T. Hla. 2005. The prostaglandin E_2 receptor EP2 is required for cyclooxygenase 2-mediated mammary hyperplasia. *Cancer Res.* 65: 4496–4499.
21. Mann, J. R., and R. N. DuBois. 2004. Cyclooxygenase-2 and gastrointestinal cancer. *Cancer J.* 10: 145–152.
22. Chun, K. S., and Y. J. Surh. 2004. Signal transduction pathways regulating cyclooxygenase-2 expression: potential molecular targets for chemoprevention. *Biochem. Pharmacol.* 68: 1089–1100.
23. Dannenberg, A. J., S. M. Lippman, J. R. Mann, K. Subbaramaiah, and R. N. DuBois. 2005. Cyclooxygenase-2 and epidermal growth factor receptor: pharmacologic targets for chemoprevention. *J. Clin. Oncol.* 23: 254–266.
24. Basu, G. D., L. B. Pathangey, T. L. Tinder, M. LaGioia, S. J. Gendler, and P. Mukherjee. 2004. COX-2 inhibitor induces apoptosis in breast cancer cells in an in vivo model of spontaneous metastatic breast cancer. *Mol. Cancer Res.* 2: 632–642.
25. Munn, D. H., and A. L. Mellor. 2004. IDO and tolerance to tumors. *Trends Mol. Med.* 10: 15–18.
26. Uyttenhove, C., L. Pilotte, I. Theate, V. Stroobant, D. Colau, N. Parmentier, T. Boon, and B. J. Van den Eynde. 2003. Evidence for a tumoral immune resistance mechanism based on tryptophan degradation by indoleamine 2,3-dioxygenase. *Nat. Med.* 9: 1269–1274.
27. Mellor, A. L., and D. H. Munn. 1999. Tryptophan catabolism and T-cell tolerance: immunosuppression by starvation? *Immunol. Today* 20: 469–473.
28. Kai, S., S. Goto, K. Tahara, A. Sasaki, K. Kawano, and S. Kitano. 2003. Inhibition of indoleamine 2,3-dioxygenase suppresses NK cell activity and accelerates tumor growth. *J. Exp. Ther. Oncol.* 3: 336–345.
29. Hwu, P., M. X. Du, R. Lapointe, M. Do, M. W. Taylor, and H. A. Young. 2000. Indoleamine 2,3-dioxygenase production by human dendritic cells results in the inhibition of T cell proliferation. *J. Immunol.* 164: 3596–3599.
30. Mellor, A. L., and D. H. Munn. 2004. IDO expression by dendritic cells: tolerance and tryptophan catabolism. *Nat. Rev. Immunol.* 4: 762–774.
31. Frumento, G., R. Rotondo, M. Tonetti, and G. B. Ferrara. 2001. T cell proliferation is blocked by indoleamine 2,3-dioxygenase. *Transplant. Proc.* 33: 428–430.
32. Mellor, A. L., D. B. Keskin, T. Johnson, P. Chandler, and D. H. Munn. 2002. Cells expressing indoleamine 2,3-dioxygenase inhibit T cell responses. *J. Immunol.* 168: 3771–3776.
33. Munn, D. H., M. Zhou, J. T. Attwood, I. Bondarev, S. J. Conway, B. Marshall, C. Brown, and A. L. Mellor. 1998. Prevention of allogeneic fetal rejection by tryptophan catabolism. *Science* 281: 1191–1193.
34. Miki, T., H. Sun, Y. Lee, A. Tandin, A. M. Kovscek, V. Subbotin, J. J. Fung, and L. A. Valdivia. 2001. Blockade of tryptophan catabolism prevents spontaneous tolerogenicity of liver allografts. *Transplant. Proc.* 33: 129–130.

35. Takikawa, O., R. Yoshida, R. Kido, and O. Hayaishi. 1986. Tryptophan degradation in mice initiated by indoleamine 2,3-dioxygenase. *J. Biol. Chem.* 261: 3648–3653.
36. Muller, A. J., J. B. Duhadaway, P. S. Donover, E. Sutanto-Ward, and G. C. Prendergast. 2005. Inhibition of indoleamine 2,3-dioxygenase, an immunoregulatory target of the cancer suppression gene Bin1, potentiates cancer chemotherapy. *Nat. Med.* 11: 312–319.
37. Yoshida, R., S. W. Park, H. Yasui, and O. Takikawa. 1988. Tryptophan degradation in transplanted tumor cells undergoing rejection. *J. Immunol.* 141: 2819–2823.
38. Takikawa, O., A. Habara-Ohkubo, and R. Yoshida. 1990. IFN-γ is the inducer of indoleamine 2,3-dioxygenase in allografted tumor cells undergoing rejection. *J. Immunol.* 145: 1246–1250.
39. Friberg, M., R. Jennings, M. Alsarraj, S. Dessureault, A. Cantor, M. Extermann, A. L. Mellor, D. H. Munn, and S. J. Antonia. 2002. Indoleamine 2,3-dioxygenase contributes to tumor cell evasion of T cell-mediated rejection. *Int. J. Cancer* 101: 151–155.
40. Guy, C. T., R. D. Cardiff, and W. J. Muller. 1992. Induction of mammary tumors by expression of polyomavirus middle T oncogene: a transgenic mouse model for metastatic disease. *Mol. Cell. Biol.* 12: 954–961.
41. Cardiff, R. D., and W. J. Muller. 1993. Transgenic mouse models of mammary tumorigenesis. *Cancer Surv.* 16: 97–113.
42. Maglione, J. E., D. Moghanaki, L. J. Young, C. K. Manner, L. G. Ellies, S. O. Joseph, B. Nicholson, R. D. Cardiff, and C. L. MacLeod. 2001. Transgenic Polyoma middle-T mice model premalignant mammary disease. *Cancer Res.* 61: 8298–8305.
43. Xia, J., Y. Tanaka, S. Koido, C. Liu, P. Mukherjee, S. J. Gendler, and J. Gong. 2003. Prevention of spontaneous breast carcinoma by prophylactic vaccination with dendritic/tumor fusion cells. *J. Immunol.* 170: 1980–1986.
44. Inaba, K., M. Inaba, N. Romani, H. Aya, M. Deguchi, S. Ikehara, S. Muramatsu, and R. M. Steinman. 1992. Generation of large numbers of dendritic cells from mouse bone marrow cultures supplemented with granulocyte/macrophage colony-stimulating factor. *J. Exp. Med.* 176: 1693–1702.
45. Simpson-Herrerns, L., and H. H. Lloyd. 1970. Kinetic parameters and growth curves for experimental tumor systems. *Cancer Chemother. Rep.* 54: 143–174.
46. Abramoff, M. D., P. J. Magelhaes, and S. J. Ram. 2004. Image processing with Image. *J. Biophotonics Int.* 11: 36–42.
47. Travers, M. T., I. F. Gow, M. C. Barber, J. Thomson, and D. B. Shennan. 2004. Indoleamine 2,3-dioxygenase activity and L-tryptophan transport in human breast cancer cells. *Biochim. Biophys. Acta* 1661: 106–112.
48. Basu, G. D., L. B. Pathangey, T. L. Tinder, S. J. Gendler, and P. Mukherjee. 2005. Mechanisms underlying the growth inhibitory effects of COX-2 inhibitor in human breast cancer cells. *Breast Cancer Res.* 7: 422–435.
49. Cully, M., H. You, A. J. Levine, and T. W. Mak. 2006. Beyond PTEN mutations: the PI3K pathway as an integrator of multiple inputs during tumorigenesis. *Nat. Rev. Cancer* 6: 184–192.
50. Lai, G. H., Z. Zhang, and A. E. Sirica. 2003. Celecoxib acts in a cyclooxygenase-2-independent manner and in synergy with emodin to suppress rat cholangiocarcinoma growth in vitro through a mechanism involving enhanced Akt inactivation and increased activation of caspases-9 and -3. *Mol. Cancer Ther.* 2: 265–271.
51. Soengas, M. S., and S. W. Lowe. 2003. Apoptosis and melanoma chemoresistance. *Oncogene* 22: 3138–3151.
52. Grohmann, U., F. Fallarino, R. Bianchi, C. Orabona, C. Vacca, M. C. Fioretti, and P. Puccetti. 2003. A defect in tryptophan catabolism impairs tolerance in nonobese diabetic mice. *J. Exp. Med.* 198: 153–160.
53. Munn, D. H., E. Shafizadeh, J. T. Attwood, I. Bondarev, A. Pashine, and A. L. Mellor. 1999. Inhibition of T cell proliferation by macrophage tryptophan catabolism. *J. Exp. Med.* 189: 1363–1372.
54. Takikawa, O., T. Kuroiwa, F. Yamazaki, and R. Kido. 1988. Mechanism of interferon-γ action: characterization of indoleamine 2,3-dioxygenase in cultured human cells induced by interferon-γ and evaluation of the enzyme-mediated tryptophan degradation in its anticellular activity. *J. Biol. Chem.* 263: 2041–2048.
55. Baars, P. A., L. M. Ribeiro Do Couto, J. H. Leusen, B. Hooibrink, T. W. Kuijpers, S. M. Lens, and R. A. van Lier. 2000. Cytolytic mechanisms and expression of activation-regulating receptors on effector-type $CD8^+CD45RA^+CD27^-$ human T cells. *J. Immunol.* 165: 1910–1917.
56. Bui, J. D., L. N. Carayannopoulos, L. L. Lanier, W. M. Yokoyama, and R. D. Schreiber. 2006. IFN-dependent down-regulation of the NKG2D ligand H60 on tumors. *J. Immunol.* 176: 905–913.
57. Yang, X., Y. Chu, Y. Wang, Q. Guo, and S. Xiong. 2006. Vaccination with IFN-inducible T cell α chemoattractant (ITAC) gene-modified tumor cell attenuates disseminated metastases of circulating tumor cells. *Vaccine* 24: 2966–2974.
58. Kim, C. H., M. J. Hong, S. D. Park, C. K. Kim, M. Y. Park, H. J. Sohn, H. I. Cho, T. G. Kim, and Y. K. Hong. 2006. Enhancement of anti-tumor immunity specific to murine glioma by vaccination with tumor cell lysate-pulsed dendritic cells engineered to produce interleukin-12. *Cancer Immunol. Immunother.* 55: 1–11.
59. Braun, D., R. S. Longman, and M. L. Albert. 2005. A two-step induction of indoleamine 2,3-dioxygenase (IDO) activity during dendritic-cell maturation. *Blood* 106: 2375–2381.
60. von Bergwelt-Baildon, M. S., A. Popov, T. Saric, J. M. Chemnitz, S. Classen, M. S. Stoffel, F. Fiore, U. Roth, M. Beyer, S. Debey, et al. 2006. CD25 and indoleamine 2,3-dioxygenase are upregulated by prostaglandin E_2 and expressed by tumor-associated dendritic cells in vivo:additional mechanisms of T cell inhibition. *Blood. In press.*
61. Half, E., X. M. Tang, K. Gwyn, A. Sahin, K. Wathen, and F. A. Sinicrope. 2002. Cyclooxygenase-2 expression in human breast cancers and adjacent ductal carcinoma in situ. *Cancer Res.* 62: 1676–1681.
62. Ristimaki, A., A. Sivula, J. Lundin, M. Lundin, T. Salminen, C. Haglund, H. Joensuu, and J. Isola. 2002. Prognostic significance of elevated cyclooxygenase-2 expression in breast cancer. *Cancer Res.* 62: 632–635.